



OPEN

Preparation and characterization of graphitic carbon nitride-supported L-arginine as a highly efficient and recyclable catalyst for the one-pot synthesis of condensation reactions

Hossein Ghafuri[✉], Zeinab Tajik, Nastaran Ghanbari & Peyman Hanifehnejad

In this work, graphitic carbon nitride-supported L-arginine (g-C₃N₄@L-arginine) nanocatalyst was synthesized and evaluated using FT-IR, EDX, XRD, TGA, and FESEM analyses. The performance of the prepared nanocatalyst was examined in the synthesis of 1,4-dihydropyridine, 4H-chromene, and 2,3-dihydro quinazoline derivatives. The novel g-C₃N₄@L-arginine nanocatalyst showed high thermal stability, easy separation from reaction media, the capability to be used in various multicomponent reactions, and acceptable reusability.

These days, most chemical processes are carried out in the presence of catalysts. Among various catalysts, supported catalysts have more application than other catalysts. Synthesis of this class of catalysts requires a support with high surface area for the adequate dispersion of primary catalyst. For this reason, using a suitable support is of high importance in the synthesis of such catalysts^{1–4}.

Graphitic carbon nitride (g-C₃N₄) can be used as a metal-free catalyst or catalyst support due to its excellent properties and exceptional performance. g-C₃N₄ sheets are an important class of conjugated polymers for the synthesis of new heterogeneous catalysts due to their unique electronic band structure, excellent physical, chemical, and thermal stability, high abrasion resistance, high hardness, low density, versatile performance, low synthesis cost, and recyclability^{5,6}. On the other hand, amino acids are one of the most interesting catalyst substrates due to their unique structure⁷. Arginine is one of the main and semi-essential amino acids in the body of living organisms with advantages such as nontoxicity, ability to easily bind to catalytic support, and low cost for the preparation of acidic catalysts. In addition, acidic catalysts play an important role in the synthesis of organic compounds. Heterocyclic compounds are one of the best candidates in organic synthesis and pharmaceutical chemistry. They are mainly used as medicines, chemicals, veterinary products, disinfectants, expanders, and antioxidants⁸.

The use of inexpensive and non-toxic reagents as well as low waste production is of great importance in green chemistry reactions. Hence, multicomponent reactions (MCRs) are considered as a useful method for the synthesis of heterocyclic organic molecules. Significant advantages of MCRs are the elimination of intermediates, short reaction times, high reaction yield, and easy separation of products^{9–12}. Compounds such as 1,4-dihydropyridine, tetrahydro-4H-chromenes, and dihydroquinazolines, which have high medicinal activity, are synthesized by MCRs.

Dihydropyridines are divided into two classes; symmetrical and asymmetrical. The latter is synthesized by the reaction of an aldehyde, 2 mmol of two different β -keto esters, and a nitrogen donor such as ammonium acetate or ammonia. The product of the initial reaction is dihydropyridine that can later be converted to pyridine. These compounds are an important class of antihypertensive drugs, vasodilators, hypnotic, anti-tumor^{13,14}, anti-inflammatory^{15,16}, anti-diabetic, anti-anxiety, anti-mutation, and are known as calcium channel blockers¹⁷.

Tetrahydro-4H-chromenes are an important class of heterocyclic compounds with simple structure and low side effects. They are synthesized by the single-step condensation of aldehydes with malononitrile and

Catalysts and Organic Synthesis Research Laboratory, Department of Chemistry, Iran University of Science and Technology, 16846-13114 Tehran, Iran. ✉email: ghafuri@iust.ac.ir

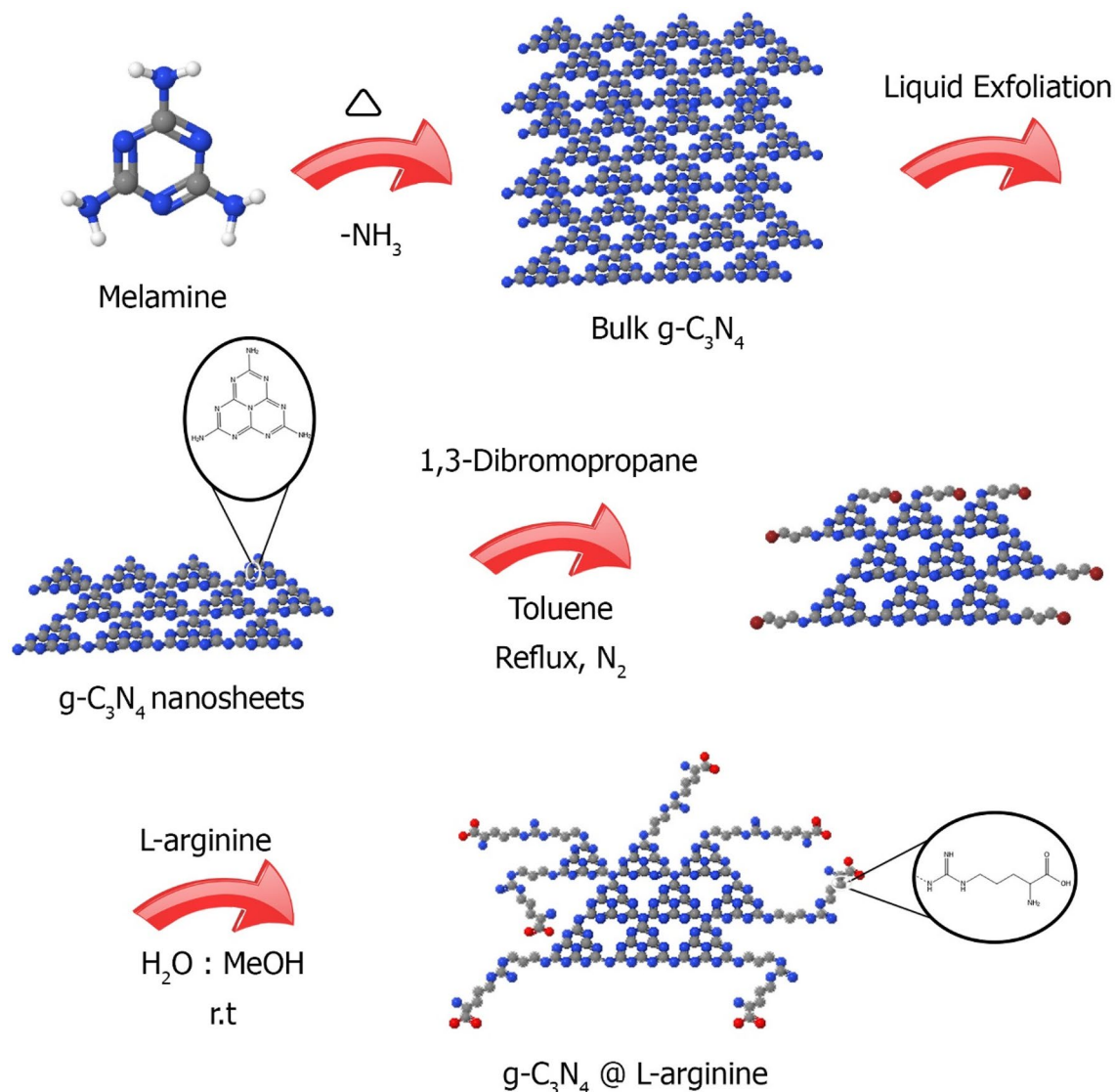


Figure 1. Synthesis of g-C₃N₄@L-arginine.

dimedone¹⁸. In addition, their derivatives have important activities such as anticancer, antiviral, anti-inflammatory, antibacterial, antifungal, antioxidant, and anticoagulant. They are also used as cognitive enhancers to treat Alzheimer's disease^{19,20}.

Dihydroquinazolines are the building blocks of about 150 natural alkaloids which are prepared by the reaction between aldehydes, isotonic anhydride, and ammonium acetate. Moreover, they have a range of pharmaceutical and biological activities such as anti-inflammatory, antimicrobial, antibacterial, anticancer, and antiviral activities^{21,22}. Hence, many efforts have been made to synthesize such high-yield compounds. There are various methods for the synthesis of these compounds using different catalysts such as MCM-41@Schiff base-Co (OAC)₂²³, Yb (NPf₂)₃²⁴, MCM-41@serine@Cu(II)²⁵, titanium silicon oxide nanopowder²⁶, Y(NO₃)₃·6H₂O²⁷, etc. despite their numerous advantages, they have some limitations such as long reaction time, expensive reagents, and the possibility of their contamination in final products.

In this paper, new g-C₃N₄@L-arginine catalyst with the ability to perform various multi-combination reactions with high yield, short reaction time, recyclability, and easy separation from the reaction mixture is synthesized and examined (Fig. 1).

Results and discussion

The g-C₃N₄@L-arginine synthesis process consists of three main steps, as shown in Fig. 1. The first step is the synthesis of nanosheet g-C₃N₄ from melamine, which melamine was polymerized to bulk g-C₃N₄, then nanosheet g-C₃N₄ is synthesized by liquid exfoliation and sonication. In the second step, g-C₃N₄ nanosheets were modified by 1,3-dibromopropane at 100 °C for 24 h under nitrogen atmosphere. Finally, the g-C₃N₄@L-arginine was obtained via the reaction between L-arginine and modified g-C₃N₄ nanosheets. In this work, various techniques such as FTIR, EDX, XRD, FESEM, and TGA have been used to identify and characterize the novel nanocatalyst.

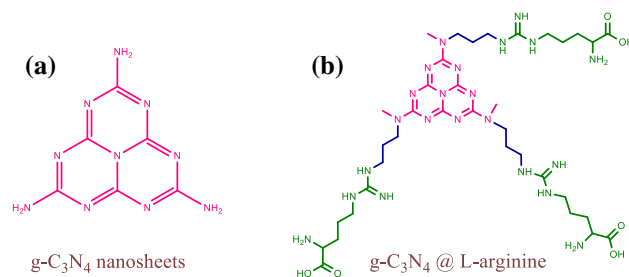


Figure 2. Nanosheets $g\text{-C}_3\text{N}_4$, (a) and $g\text{-C}_3\text{N}_4 @ \text{L-arginine}$ (b).

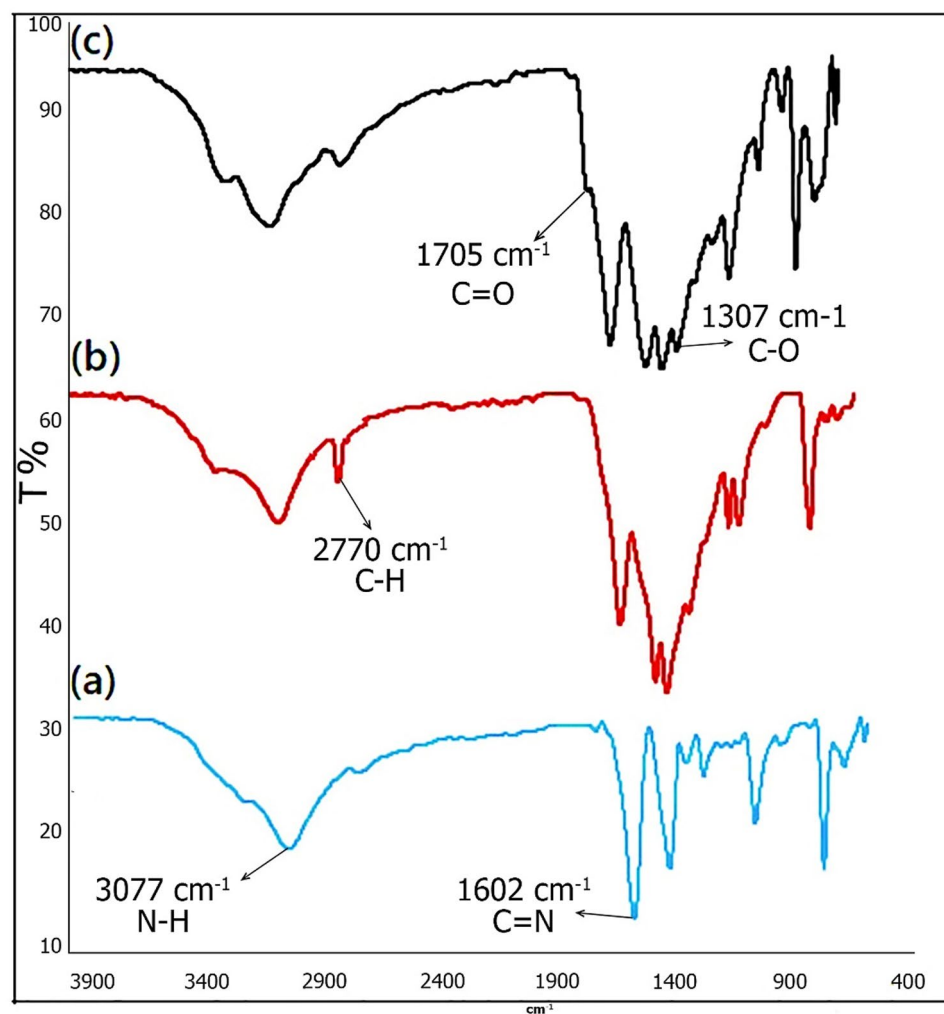


Figure 3. FT-IR spectra of (a) nanosheets $g\text{-C}_3\text{N}_4$, (b) modified $g\text{-C}_3\text{N}_4$, (c) $g\text{-C}_3\text{N}_4 @ \text{L-arginine}$.

FTIR spectra of $g\text{-C}_3\text{N}_4$ nanosheets (Fig. 2a) and $g\text{-C}_3\text{N}_4 @ \text{L-arginine}$ nanocatalyst (Fig. 2b) are shown in Fig. 2. The strong and broad peak in the range of 3000–3300 cm^{-1} is related to stretching vibration of N–H bonds, breadth peak can be assigned to N–H groups involved in H-bonding or the presence of O–H groups due to water adsorption by nanosheets $g\text{-C}_3\text{N}_4$ ^{28,29}. The stretching vibration peak of C=N can be observed at 1602 cm^{-1} . The peaks at 1303 and 1082 cm^{-1} are attributed to the stretching vibration of C–N bonds formed between triazine and N–H groups, while the stretching vibration of C–N bonds in the ring is easily visible at 1448 and 1379 cm^{-1} ^{29,30}. In addition, the peak at 786 cm^{-1} is associated with the vibration of tri-s-triazine units¹ (Fig. 3a). Figure 3b shows that the $g\text{-C}_3\text{N}_4$ nanosheets has been modified with 1,3-dibromopropane; the peak at 3000–2800 cm^{-1} is related to C–H stretching vibration.

The spectrum of $g\text{-C}_3\text{N}_4 @ \text{L-arginine}$ is presented in Fig. 3c in which the existence of L-arginine on the surface of $g\text{-C}_3\text{N}_4$ nanosheets can be confirmed based on the 1705 cm^{-1} and 1307 cm^{-1} peaks relating to the stretching

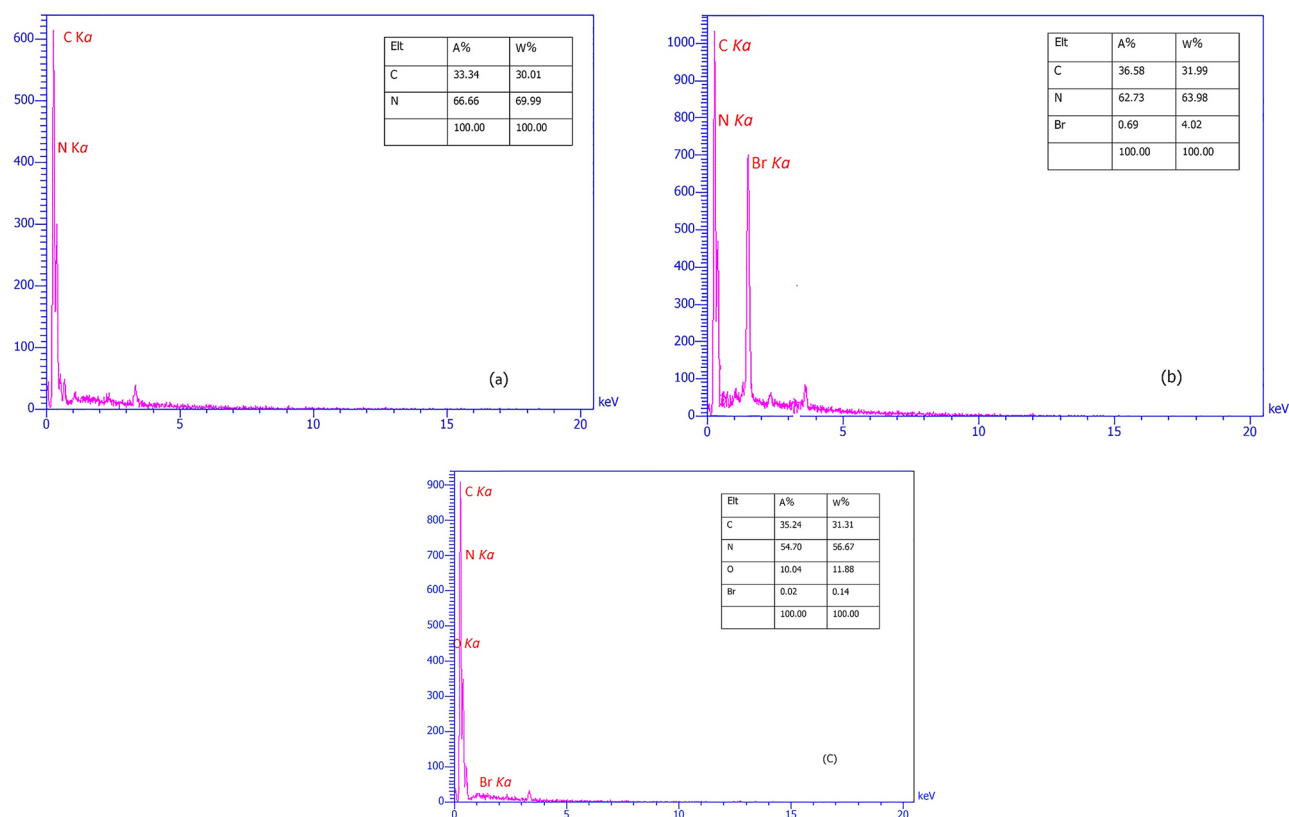


Figure 4. EDX spectrum of (a) nanosheets $g\text{-C}_3\text{N}_4$, (b) modified $g\text{-C}_3\text{N}_4$, (c) $g\text{-C}_3\text{N}_4@L\text{-arginine}$.

vibration of C=O and C-O bonds, respectively. O-H and C-H bonds already existed in the structure of modified nanosheets $g\text{-C}_3\text{N}_4$.

The presence of carbon and nitrogen elements in the structure of $g\text{-C}_3\text{N}_4$ nanosheets is visible in Fig. 4a. The presence of Br element in the structure proves that $g\text{-C}_3\text{N}_4$ nanosheets have been modified by 1,3-dibromopropane (Fig. 4b). Finally, the presence of carbon, nitrogen, and oxygen in the final structure ($g\text{-C}_3\text{N}_4@L\text{-arginine}$) confirmed the synthesis of $g\text{-C}_3\text{N}_4@L\text{-arginine}$ nanocatalyst (Fig. 4c).

The morphology of $g\text{-C}_3\text{N}_4$ nanosheets and $g\text{-C}_3\text{N}_4@L\text{-arginine}$ was investigated by FE-SEM. Figure 5a-d shows FE-SEM images of $g\text{-C}_3\text{N}_4$ nanosheets. As shown in Figs. 5a-c, the $g\text{-C}_3\text{N}_4$ nanosheets have a smooth and flat surface, while in Fig. 5d, $g\text{-C}_3\text{N}_4$ nanosheets are irregular and connected together. FE-SEM images of $g\text{-C}_3\text{N}_4@L\text{-arginine}$ are shown in Fig. 5e-h. It can be seen from Fig. 5e-g that $g\text{-C}_3\text{N}_4$ nanosheets have a flake-like morphology with a relatively rough surface, mainly due to the presence of L-arginine on the surface of $g\text{-C}_3\text{N}_4$ nanosheets. In Fig. 5h, more irregular-shape $g\text{-C}_3\text{N}_4$ nanosheets with tiny particles on the surface are observed, which again confirms the deposition of L-arginine on the $g\text{-C}_3\text{N}_4$ nanosheets.

XRD patterns of $g\text{-C}_3\text{N}_4$ nanosheets and $g\text{-C}_3\text{N}_4@L\text{-arginine}$ are shown in Figs. 6a and 4b, respectively. The diffraction peaks at $2\theta = 27.69$ and 15.96 (Fig. 6a) prove the successful synthesis of $g\text{-C}_3\text{N}_4$ nanosheets^{1,7,28}, while the diffraction peaks at $2\theta = 6.07$, 10.85 , 12.21 , 23.60 , and 30.97 (Fig. 6b) correspond to L-arginine (JCPDS card no. 00-004-0180), confirming the presence of L-arginine on the surface of $g\text{-C}_3\text{N}_4$ nanosheets.

Figure 7 shows the thermal stability of the synthesized $g\text{-C}_3\text{N}_4@L\text{-arginine}$ in the range of $50\text{--}800\text{ }^\circ\text{C}$. As can be seen, the weight ratio has gradually decreased by increasing the temperature from 100 to $200\text{ }^\circ\text{C}$, which is most likely related to the removal of water absorbed on the surface of $g\text{-C}_3\text{N}_4@L\text{-arginine}$. Then, another weight loss is observed in the range of 200 to $400\text{ }^\circ\text{C}$, which is attributed to the separation of L-arginine from the structure. Finally, there is another weight loss in the range of 400 to $700\text{ }^\circ\text{C}$ due to the decomposition of $g\text{-C}_3\text{N}_4$ nanosheets³¹.

Model reactions. The performance of the prepared $g\text{-C}_3\text{N}_4@L\text{-arginine}$ nanocatalyst was evaluated for the synthesis of 1,4-dihydropyridine, 4*H*-chromene, and 2,3-dihydro quinazoline derivatives. For this purpose, various parameters such as reaction time, catalyst concentration, and the solvent were examined (Table 1). The reaction of 4-chlorobenzaldehyde (1 mmol), ethyl acetoacetate (1 mmol), dimedone (1 mmol), and ammonium acetate (1 mmol) for the synthesis of 1,4-dihydropyridine derivatives, the reaction of 4-chlorobenzaldehyde (1 mmol), dimedone (1 mmol), and malononitrile (1 mmol) for the synthesis of 4*H*-chromene derivatives, and the reaction of 4-chlorobenzaldehyde (1 mmol), isotonic anhydride (1 mmol), and ammonium acetate (1 mmol) for the synthesis of 2,3-dihydro quinazoline derivatives were considered as model reactions with and without $g\text{-C}_3\text{N}_4@L\text{-arginine}$ nanocatalyst under different conditions. The reaction progress was monitored by Thin-layer

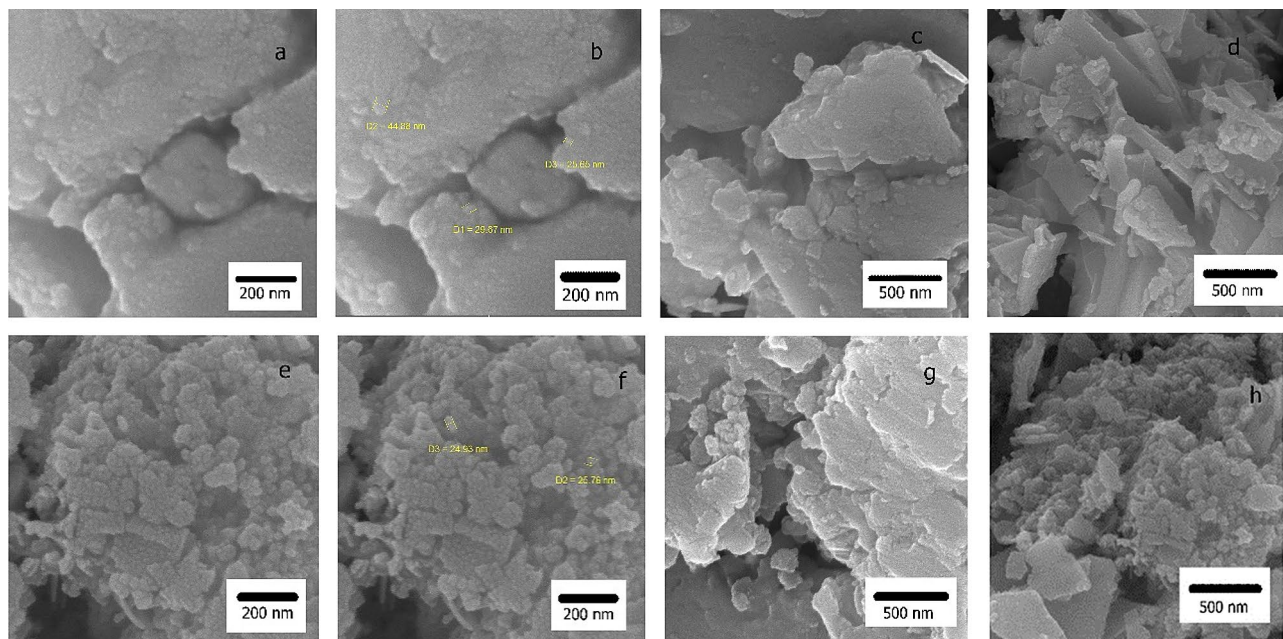


Figure 5. FE-SEM image of nanosheets g-C₃N₄ (a, b, c, and d), and g-C₃N₄@L-arginine (e, f, g, h).

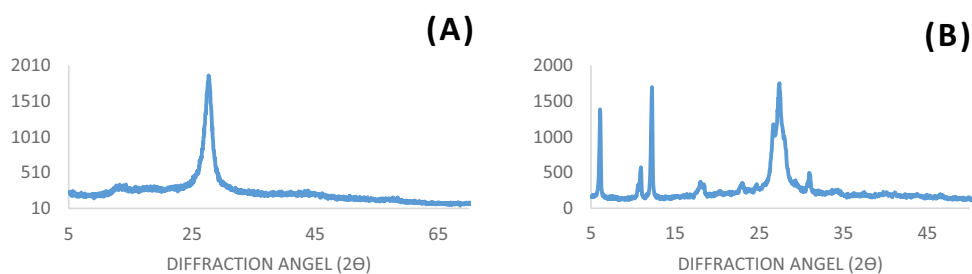


Figure 6. XRD pattern of (a) nanosheets g-C₃N₄, (b) g-C₃N₄@L-arginine.

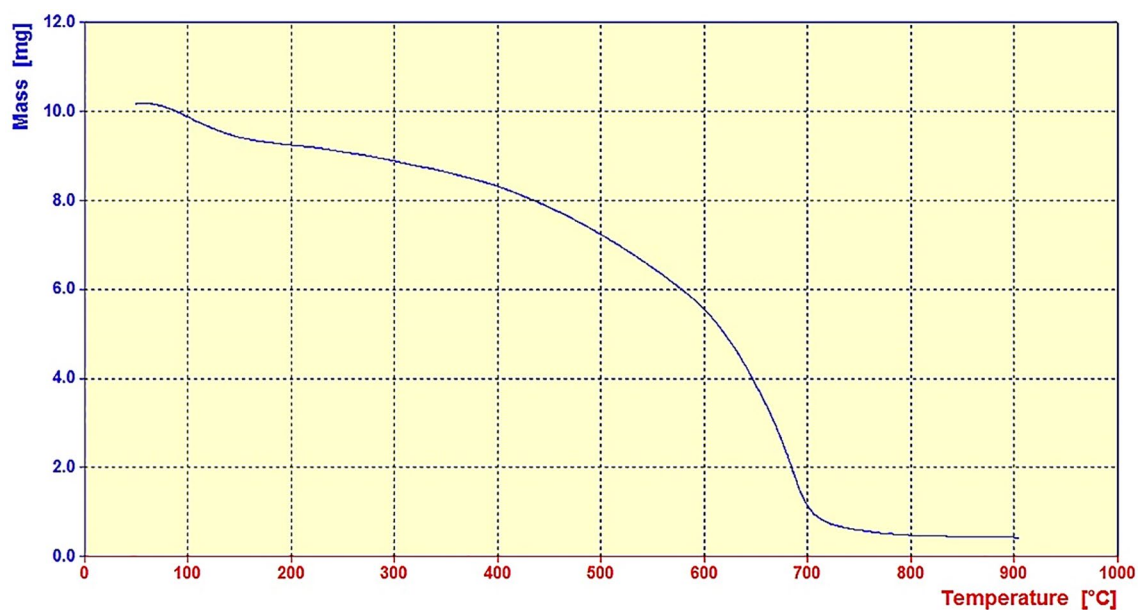


Figure 7. TGA analysis of g-C₃N₄@L-arginine.

| Entry | Catalyst | Catalyst loading (mg) | Solvent | Time (min) | Temperature (°C) | Yield (%) | | |
|-------|---|-----------------------|---------------------------------|------------|------------------|---------------------------|---------------------------|---------------------------|
| | | | | | | Reaction (1) ^a | Reaction (2) ^b | Reaction (3) ^c |
| 1 | – | – | EtOH | 60 | r.t | – | – | – |
| 2 | – | – | EtOH | 60 | Reflux | – | – | – |
| 3 | g-C ₃ N ₄ @L-arginine | 1.00 | EtOH | 15 | Reflux | 53 | 60 | 57 |
| 4 | g-C ₃ N ₄ @L-arginine | 10.00 | EtOH | 15 | Reflux | 85 | 90 | 87 |
| 5 | g-C ₃ N ₄ @L-arginine | 20.00 | EtOH | 15 | Reflux | 94 | 97 | 96 |
| 6 | g-C ₃ N ₄ @L-arginine | 30.00 | EtOH | 15 | Reflux | 95 | 98 | 96 |
| 7 | g-C ₃ N ₄ @L-arginine | 20.00 | EtOH | 10 | Reflux | 89 | 97 | 93 |
| 8 | g-C ₃ N ₄ @L-arginine | 20.00 | EtOH | 20 | Reflux | 95 | 98 | 93 |
| 9 | g-C ₃ N ₄ @L-arginine | 20.00 | EtOH | 30 | Reflux | 96 | 98 | 94 |
| 10 | g-C ₃ N ₄ @L-arginine | 20.00 | CH ₂ Cl ₂ | 15 | Reflux | 54 | 67 | 60 |
| 11 | g-C ₃ N ₄ @L-arginine | 20.00 | DMF | 15 | Reflux | 52 | 56 | 55 |
| 12 | g-C ₃ N ₄ @L-arginine | 20.00 | H ₂ O | 15 | Reflux | 75 | 78 | 77 |
| 13 | g-C ₃ N ₄ @L-arginine | 20.00 | EtOH | 15 | r.t | 57 | 66 | 68 |

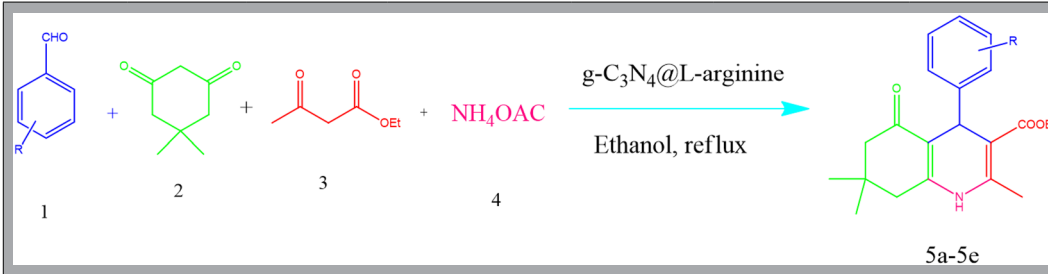
Table 1. Optimization of different parameters for model reactions 1 to 3. ^aReaction of 4-chlorobenzaldehyde (1 mmol), ethyl acetoacetate (1 mmol), dimedone (1 mmol), and ammonium acetate (1 mmol) for the synthesis of 1,4-dihydropyridine. ^bReaction of 4-chlorobenzaldehyde (1 mmol), dimedone (1 mmol), and malononitrile (1 mmol) for the synthesis of 4H-chromene. ^cReaction of 4-chlorobenzaldehyde (1 mmol), isotonic anhydride (1 mmol), and ammonium acetate (1 mmol) for the synthesis of 2,3-dihydroquinazoline.

chromatography (TLC). As can be seen in Table 1 (entries 1 and 2), no progress was observed for the model reactions without nanocatalyst. By introducing 1.00 mg of g-C₃N₄@L-arginine (Table 1, entry 3), however, the model reactions occurred easily. Then, the influence of other parameters including catalyst concentration, reaction time, and solvent were examined. As can be seen, time had not significant effect on the reaction progress, thus 15 min was considered as the optimum reaction time for all the model reactions (Table 1, entries 7, 8, and 9). Furthermore, the highest product yield was obtained using ethanol as solvent at 80 °C in the presence of 20.00 mg of g-C₃N₄@L-arginine (Table 1, entry 5).

In the following, various aldehydes were applied for the synthesis of 1,4-dihydropyridine, 4H-chromene, and 2,3-dihydro quinazoline derivatives under optimal reaction conditions. Based on model reactions that are provided in Tables 2, 3 and 4, a wide range of different derivatives of the desired multicomponent reactions were prepared with high yield.

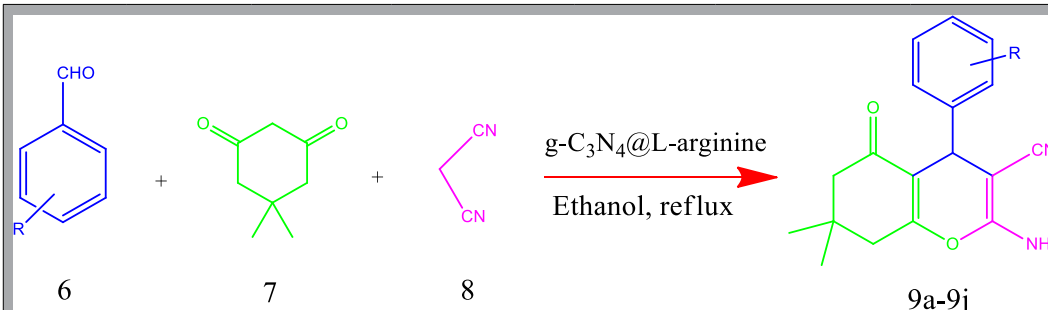
Reusability of g-C₃N₄@L-arginine nanocatalyst. According to the importance of recovery and recyclability in green chemistry, in this section, the reusability of g-C₃N₄@L-arginine was examined for the synthesis of 1,3-dihydropyridine **5b**, 4H-chromene **9b**, and 2,3-dihydroquinazoline **13b** products. For this purpose, after the first reaction (run 1), g-C₃N₄@L-arginine catalyst was separated from the reaction media, washed with ethanol, and dried in an oven at 70 °C. Then, the catalyst was reused for the next run. This was repeated for five times and the obtained yields were acceptable for catalytic reactions, and although performed reaction yields were decreased at each run bit by bit, in run 5th, the observed decrement was impressive in comparison with other runs (Fig. 8). EDX and FTIR spectra after the 5th run showed no significant changes in the primary structure of the g-C₃N₄@L-arginine nanocatalyst, as shown in Fig. 9.

Mechanistic study of the prepared nanocatalyst in the synthesis of 1,4-dihydropyridine, 4H-chromene, and 2,3-dihydro quinazoline derivatives. In Fig. 10, the suitable mechanism for the formation of 1,4-dihydropyridine, 2,3-dihydro quinazoline, and 4H-chromene derivatives are provided. In each reaction, the presence of g-C₃N₄@L-arginine can activate reactants and different intermediates. As can be seen in Fig. 10a, 1,4-dihydropyridine derivatives can be synthesized in two methods. In the first method, aldehyde and dimedone produce intermediate **I** in the presence of g-C₃N₄@L-arginine, and the intermediate **II** is formed from the reaction between ethyl acetoacetate and ammonium acetate. But in the second method, dimedone and ammonium acetate produce intermediate **III** in the presence of g-C₃N₄@L-arginine, and the reaction between ethyl acetoacetate and aldehyde forms intermediate **IV**. Both methods ultimately lead to the formation of product **V**.



| Entry | R | Product | Time (min) | Mp (°C) | Mp (°C, ref.) | Yield (%) |
|-------|-------------------|---------|------------|---------|-----------------------|-----------|
| 1 | H | 5a | 10 | 217–219 | 218–220 ¹⁷ | 95 |
| 2 | 4-Cl | 5b | 15 | 240–242 | 241–243 ¹⁷ | 94 |
| 3 | 4-OH | 5c | 20 | 230–232 | 231–232 ¹⁴ | 89 |
| 4 | 4-NO ₂ | 5d | 15 | 239–241 | 240–242 ¹⁴ | 90 |
| 5 | 4-Me | 5e | 25 | 254–256 | 250 ³² | 87 |

Table 2. Synthesis of 1,4-dihydropyridine derivatives using $g\text{-C}_3\text{N}_4@L\text{-arginine}$ nanocatalyst. **Reaction conditions:** benzaldehyde (1 mmol), ethyl acetoacetate (1 mmol), dimedone (1 mmol), and ammonium acetate (1 mmol), $g\text{-C}_3\text{N}_4@L\text{-arginine}$ (20 mg) and ethanol (7 mL) under reflux conditions.



| Entry | R | Product | Time (min) | Mp (°C) | Mp (°C, ref.) | Yield (%) |
|-------|-------------------|---------|------------|---------|-----------------------|-----------|
| 1 | H | 9a | 7 | 228–229 | 225–228 ³³ | 95 |
| 2 | 4-Cl | 9b | 10 | 210–212 | 211–213 ³³ | 97 |
| 3 | 4-NO ₂ | 9c | 15 | 178–179 | 177–179 ³⁴ | 88 |
| 4 | 2,4-Cl | 9d | 10 | 118–120 | 115–117 ²⁴ | 95 |
| 5 | 4-OH | 9e | 20 | 206–208 | 208–210 ²⁴ | 93 |
| 6 | 4-Me | 9f | 30 | 217–220 | 220–221 ³⁵ | 91 |
| 7 | 3-NO ₂ | 9g | 20 | 206–207 | 206–209 ³⁴ | 93 |
| 8 | 2-Cl | 9h | 15 | 213–214 | 211–213 ³⁵ | 96 |
| 9 | 4-CN | 9i | 25 | 184–187 | 184–186 ³⁵ | 89 |
| 10 | 4-OMe | 9j | 30 | 203–204 | 196–198 ³³ | 87 |

Table 3. Synthesis of 4H-chromene derivatives using $g\text{-C}_3\text{N}_4@L\text{-arginine}$ nanocatalyst. **Reaction conditions:** Reaction of benzaldehyde (1 mmol), dimedone (1 mmol), and malononitrile (1 mmol) $g\text{-C}_3\text{N}_4@L\text{-arginine}$ (20 mg) and ethanol (7 mL) under reflux conditions.

A suggested mechanism for the formation of 2,3-dihydro quinazoline derivatives is shown in Fig. 10b. At first, isotonic anhydride reacts with ammonium acetate in the presence of $g\text{-C}_3\text{N}_4@L\text{-arginine}$ and produces intermediate I, then aldehyde activates by $g\text{-C}_3\text{N}_4@L\text{-arginine}$ and adds to intermediate II. Finally, after removing H, the desired product IV is synthesized.

Figure 10c presents a probable method for the synthesis of 4H-chromene derivatives in the presence of $g\text{-C}_3\text{N}_4@L\text{-arginine}$. In this mechanism, intermediate I is produced from the reaction between aldehyde and dimedone. Then, addition of malononitrile leads to the formation of intermediate II. At last, product IV is obtained.

| Entry | R | Product | Time (min) | Mp (°C) | MP (°C, ref.) | Yield |
|-------|-------------------|------------|------------|---------|-----------------------|-------|
| 1 | H | 13a | 15 | 207–210 | 208–210 ²¹ | 90 |
| 2 | 4-Cl | 13b | 15 | 203–206 | 203–206 ³⁶ | 96 |
| 3 | 3-NO ₂ | 13c | 30 | 192–193 | 190–193 ²¹ | 89 |
| 4 | 4-OH | 13d | 25 | 213–215 | 213–215 ³⁶ | 87 |
| 5 | 2-Cl | 13e | 15 | 205–206 | 206–208 ²² | 95 |
| 6 | 4-Me | 13f | 25 | 200–201 | 198–201 ²² | 86 |
| 7 | 4-NO ₂ | 13g | 20 | 201–202 | 200–202 ³⁶ | 90 |
| 8 | 4-OMe | 13h | 25 | 180–182 | 178–182 ³⁶ | 87 |
| 9 | 2,4-Cl | 13i | 35 | 163–166 | 165–169 ²¹ | 94 |
| 10 | 3-OH | 13j | 30 | 212–216 | 215–217 ³⁶ | 89 |

Table 4. Synthesis of 2,3-dihydroquinazoline derivatives using g-C₃N₄@L-arginine nanocatalyst. **Reaction conditions:** benzaldehyde (1 mmol), isotonic anhydride (1 mmol), and ammonium acetate (1 mmol), C₃N₄@L-arginine (20 mg) and ethanol (7 mL) under reflux conditions.

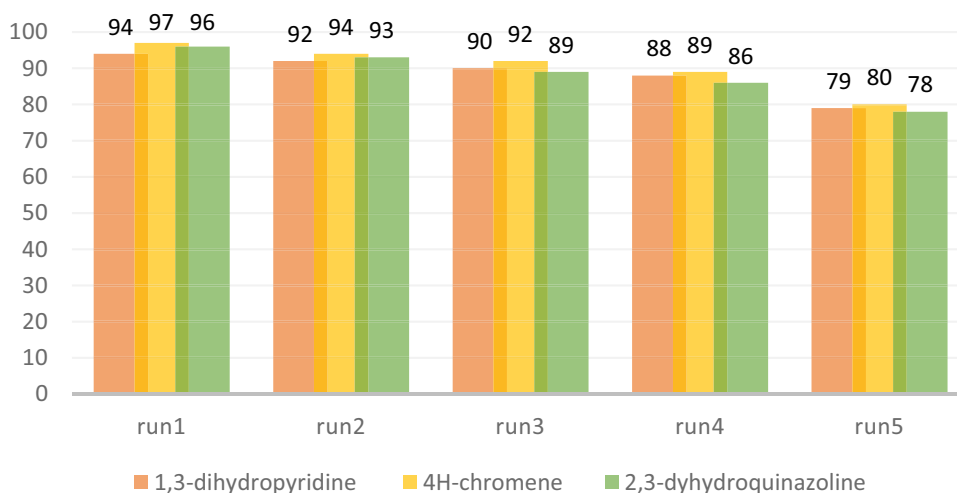


Figure 8. Examination of g-C₃N₄@L-arginine reusability in synthesis of 1, 3-dihydropyridine **5b**, 4H-chromene **9b**, and 2, 3-dihydroquinazoline **13b**.

Catalytic activity of the synthesized nanocatalyst. Tables 5, 6 and 7 show the performance of g-C₃N₄@L-arginine in comparison with the catalysts reported in the literature for the synthesis of 1,4-dihydropyridine, 4H-chromene, and 2,3-dihydroquinazoline derivatives. For this purpose, various parameters such as catalyst concentration, reaction time, reaction temperature, and reaction yield were investigated. According to the data presented in each table, g-C₃N₄@L-arginine can be considered as a unique heterogeneous nanocatalyst that can be used in a wide range of condensation reactions in addition to simple separation conditions of the reaction mixture. On the other hand, this nanocatalyst exceptionally showed higher synthesis yield at shorter reaction times.

Experimental

Reagents and apparatus. All chemicals were purchased from Merck and Sigma-Aldrich Co. Fourier Transform Infrared (FTIR) spectra were recorded on Tensor27. Nuclear Magnetic Resonance (NMR) data were acquired on a Varian-Inova 500 MHz. X-Ray Diffraction (XRD) patterns were obtained using Dron-8 diffractometer. Energy-dispersive X-ray (EDX) spectrum was recorded on Numerix DXP-X10P. Thermal gravimetric

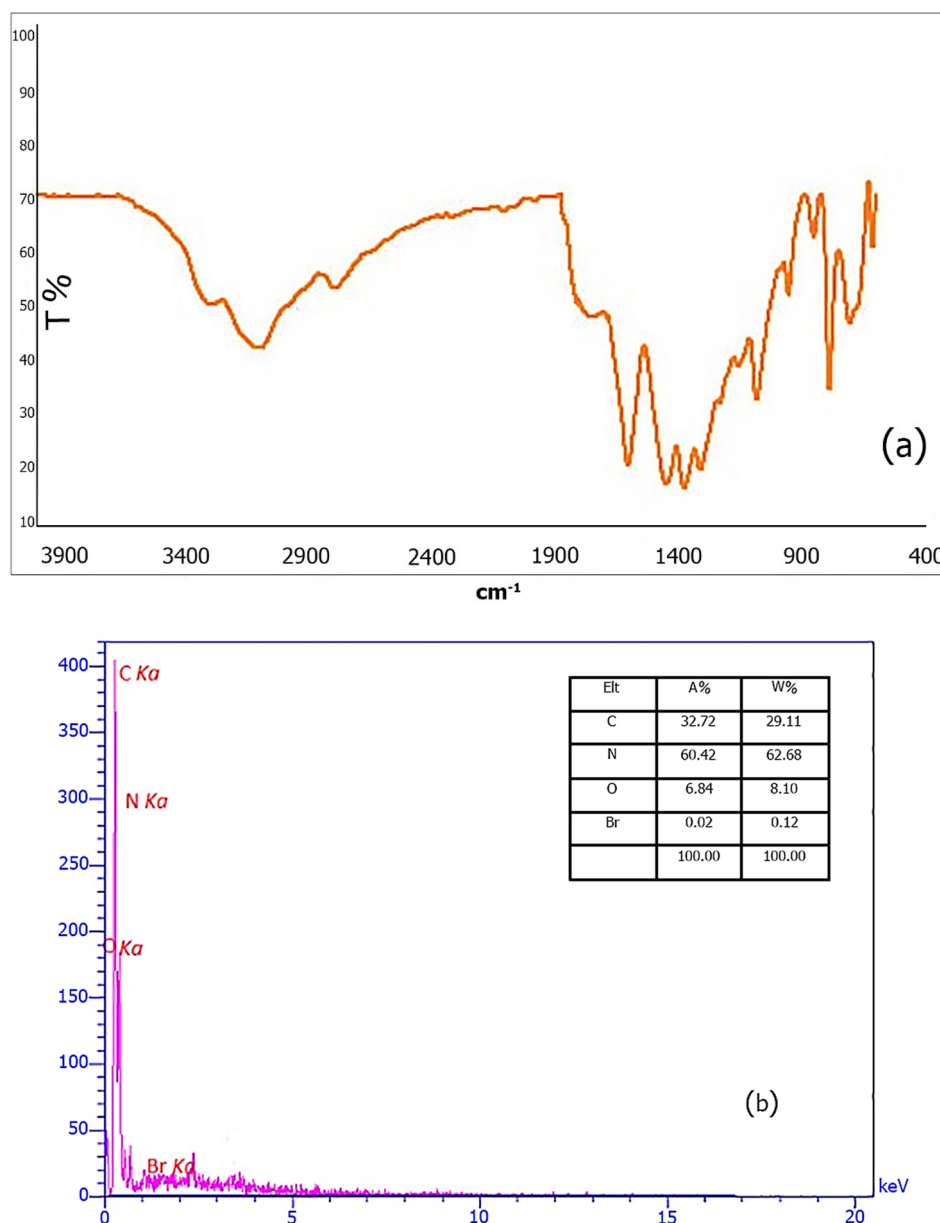


Figure 9. EDX (b) and FT-IR spectra (a) of g-C₃N₄@L-arginine after the five-times recycling.

analysis (TGA) was performed using STA 504 instrument under argon atmosphere. Field Emission Scanning Electron Microscopy (FESEM) images were recorder with TESCAN-MIRA III.

Preparation of bulk g-C₃N₄ and g-C₃N₄ nanosheets. For the synthesis of bulk g-C₃N₄, the melamine was heated at 550 °C in a furnace at the heating rate of 2.5 °C min⁻¹ in static air for 4 h. A yellow powder was obtained which was then grounded in a ball mill. For the synthesis of g-C₃N₄ nanosheets, bulk g-C₃N₄ (1.0 g) was first stirred in H₂SO₄ (20 mL) at 90 °C for 5 h. The solution was then diluted with ethanol (200 mL) and stirred again at room temperature for 2 h. The resulting product was dispersed in 100.0 mL water/isopropanol (1:1) solution and sonicated for 6 h. Finally, the formed suspension was centrifuged at 5000 rpm to separate g-C₃N₄ nanosheets.

Preparation of g-C₃N₄@L-arginine. g-C₃N₄ (1.0 g) nanosheets were dispersed in dry toluene (20.0 mL). Then, the reaction mixture was refluxed under N₂ atmosphere for 24 h after addition of 1,3-dibromopropane (2.0 mL). Finally, the product was filtered and washed with ethyl acetate, and dried at room temperature. The resulting product was dissolved in a mixture of water and methanol (1:1) followed by the addition of L-arginine (1 mmol), K₂CO₃ (1.0 mmol), and NaI (1.0 mmol). The solution was stirred at room temperature for 24 h. the reaction mixture was then washed with water and methanol and dried at room temperature.

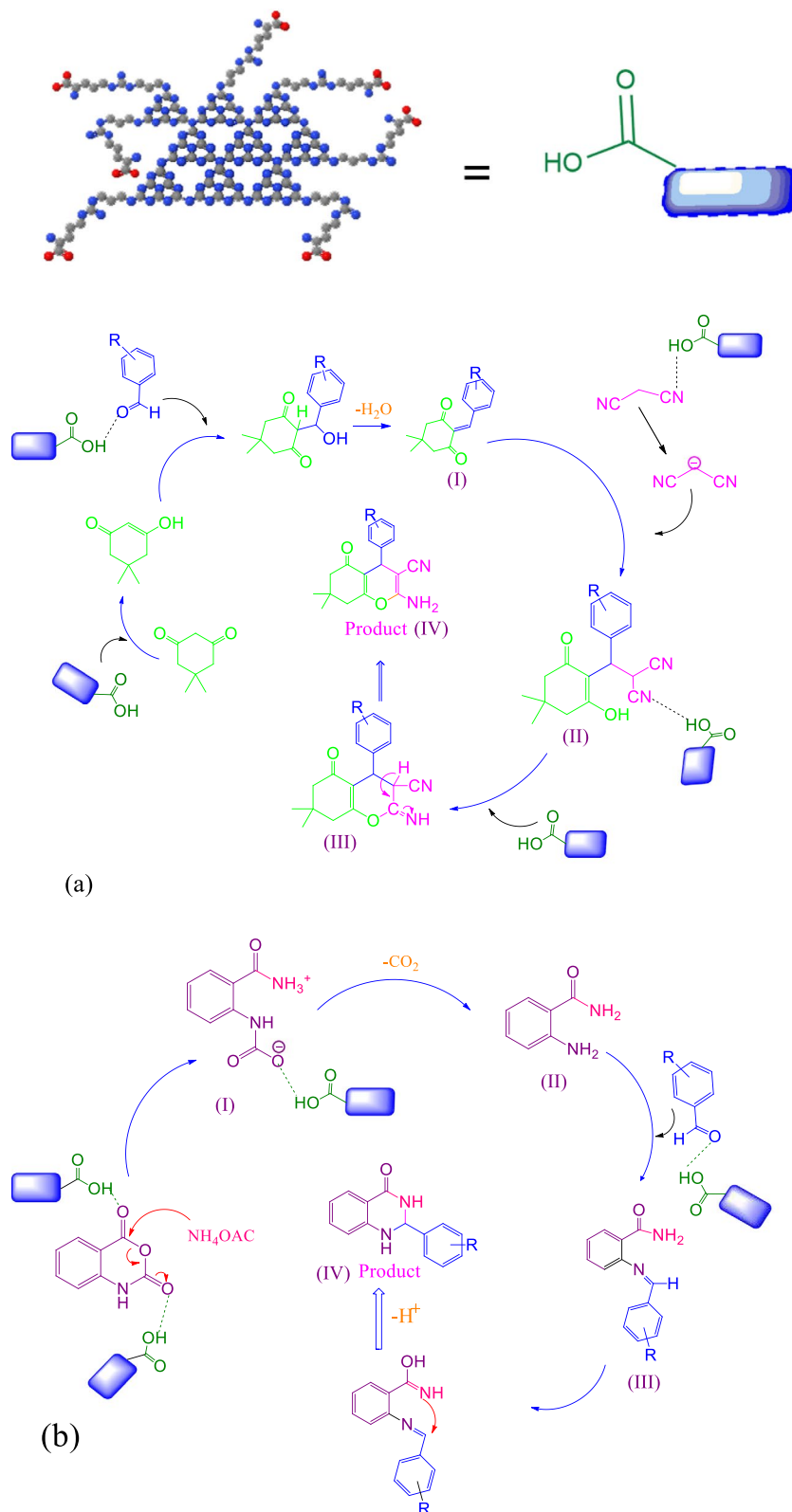


Figure 10. Proposed mechanism for synthesis of 4H-chromene derivatives (a), 2,3-dihydro quinazoline (b), and 1,4-dihydropyridine (c) by using g-C₃N₄@L-arginine.

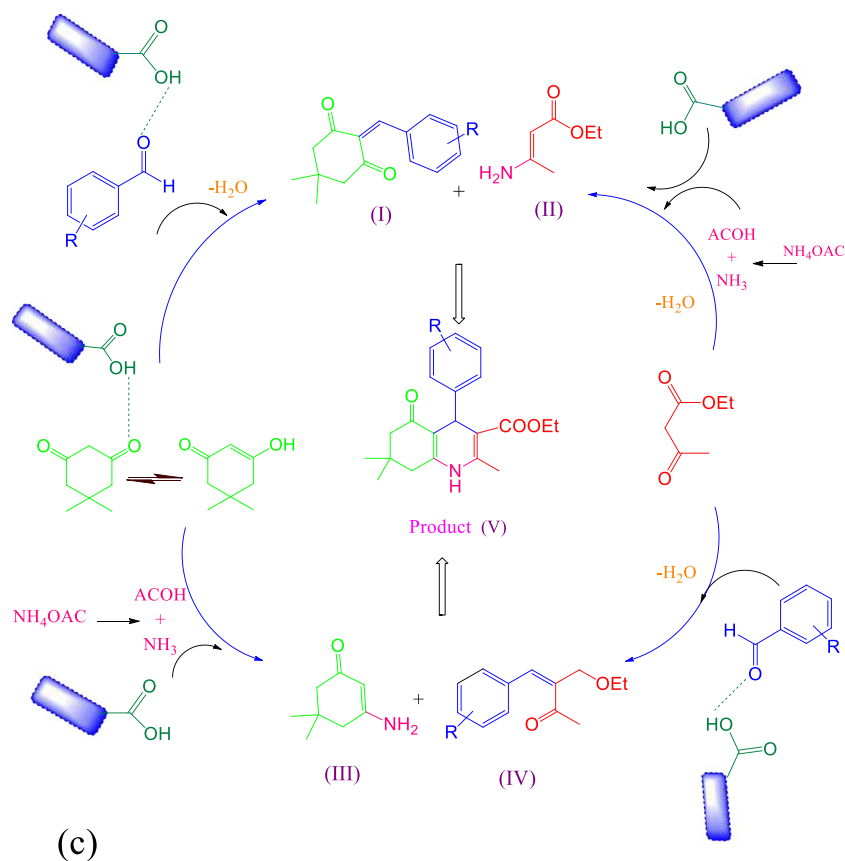


Figure 10. (continued)

| Entry | Catalyst | Solvent/temperature | Time (min) | Chromene yield (%) | Ref |
|-------|---|-----------------------------|------------|--------------------|-----------|
| 1 | Fe ₃ O ₄ @MCM-41@Zr-piperazine-MNPs | EtOH/H ₂ O/75 °C | 40 | 74 | 37 |
| 2 | AIL@MNP | Solvent-free/90 °C | 25 | 89 | 38 |
| 3 | MCM-41@Schiff base-Co(OAC) ₂ | H ₂ O/50 °C | 180 | 94 | 23 |
| 4 | Yb(NPf ₂) ₃ | EtOH/80 °C | 240 | 91 | 24 |
| 5 | g-C ₃ N ₄ @L-arginine | EtOH/reflux | 7 | 95 | This work |

Table 5. Comparison of catalytic activity of g-C₃N₄@L-arginine with other reported catalysts for the synthesis of 4H-chromene derivatives. Reaction conditions: benzaldehyde (1 mmol), dimedone (1 mmol), malononitrile (1.5 mmol), g-C₃N₄@L-arginine catalyst (20.00 mg), and ethanol (7 mL) under reflux.

| Entry | Catalyst | Solvent/temperature | Time (min) | Hantzsch yield (%) | Ref |
|-------|--|---------------------|------------|--------------------|-----------|
| 1 | BNPs @ Si(CH ₂) ₃ @NH SO ₃ H | EtOH/reflux | 25 | 95 | 39 |
| 2 | Aluminized polyborate | Solvent-free/100 °C | 15 | 94 | 14 |
| 3 | Cell-Pr-NHSO ₃ H | EtOH/reflux | 45 | 91 | 40 |
| 4 | MCM-41@serine@Cu(II) | EtOH/80 °C | 170 | 96 | 25 |
| 5 | g-C ₃ N ₄ @L-arginine | EtOH/reflux | 10 | 95 | This work |

Table 6. Comparison of catalytic activity of g-C₃N₄@L-arginine with other reported catalysts for the synthesis of 1,4-dihydropyridine derivatives: **Reaction conditions:** Reaction of benzaldehyde (1 mmol), dimedone (1 mmol), and malononitrile (1 mmol) g-C₃N₄@L-arginine (20 mg) and ethanol (7 mL) under reflux conditions.

| Entry | Catalyst | Solvent/temperature | Time (min) | Quinazoline yield (%) | Ref |
|-------|---|-------------------------|------------|-----------------------|-----------|
| 1 | Titanium silicon oxide nanopowder | H ₂ O/100 °C | 120 | 94 | 26 |
| 2 | Wang-OSO ₃ H | H ₂ O/100 °C | 24 | 84 | 22 |
| 3 | Y(NO ₃) ₃ ·6H ₂ O | CH ₃ CN | 300 | 97 | 27 |
| 4 | Montmorillonite-KSF | Solvent-free/100 °C | 150 | 93 | 41 |
| 5 | g-C ₃ N ₄ @L-arginine | EtOH/reflux | 15 | 96 | This work |

Table 7. Comparison of catalytic activity of g-C₃N₄@L-arginine with other reported catalysts for the synthesis of 2,3-dihydro quinazoline derivatives. Reaction condition: 4-chlorobenzaldehyde (1mmol), isotonic anhydride (1mmol), and ammonium acetate (1mmol), g-C₃N₄@L-arginine catalyst (20.00 mg), and ethanol (7 mL) under reflux.

General procedure for the synthesis of 1,4-dihydropyridine derivatives. A mixture of aldehyde (1.0 mmol), ethyl acetoacetate (1.0 mmol), dimedone (1.0 mmol), ammonium acetate (1.0 mmol), g-C₃N₄@L-arginine (20.0 mg), and ethanol (2.0 mL) was added in a round bottom flask and refluxed at 70 °C. When the reaction was completed (monitored by TLC), the catalyst was separated by filtration and washed with ethanol, and then to purifying the product was used recrystallization.

General procedure for the synthesis of 2,3-dihydro quinazoline derivatives. In a round bottom flask, aldehyde (1.0 mmol), isotonic anhydride (1.0 mmol), ammonium acetate (2.0 mmol), and g-C₃N₄@L-arginine (20.0 mg) were added and refluxed in ethanol (2.0 mL) at 70 °C. After reaction completion (monitored by TLC), the catalyst was removed by filtration and washed with ethanol, and then to purifying the product was used recrystallization.

General procedure for the synthesis of 4H-chromene derivatives. In a round bottom flask was added aldehyde (1.0 mmol), dimedone (1.0 mmol), malononitrile (1.0 mmol), g-C₃N₄@L-arginine (20.0 mg), and ethanol (2.0 mL). The mixture was then refluxed at 70 °C until the reaction was completed (monitored by TLC). At last, catalyst separation by filtration and washed with ethanol, and then to purifying the product was used recrystallization.

Conclusions

In summary, heterogeneous g-C₃N₄@-arginine nanocatalyst was prepared and used for the synthesis of 1,4-dihydropyridine, 4H-chromene, and 2,3-dihydro quinazoline derivatives as important products in pharmacologically active compounds. The main advantages of this nanocatalyst is its reusability, simple separation from the reaction mixture, applicability for a broad range of high efficiency condensation reactions, and short reaction time. In addition, the use of an easy and convenient method for the preparation of the nanocatalyst is another advantage of this catalyst over other reported catalysts.

Selected spectral data

Ethyl 2,7,7-trimethyl-5-oxo-4-(4-hydroxyphenyl)-1,4,5,6,7,8-hexahydroquinoline-3-carboxylate (5c). FTIR (KBr, cm⁻¹): 3270, 3194, 3071, 2957, 1678, 1645, 1481, 1377, 1214 cm⁻¹. ¹H NMR (500 MHz, DMSO): δ H (ppm) = 0.85(s, 3H, CH₃), 1.0(s, 3H, CH₃), 1.13(t, 3H, CH₃), 1.9–2.41(m, 4H, 2CH₂), 2.25(s, 3H, CH₃), 3.95–3.99(q, 2H, OCH₂), 4.73(s, 1H, Ar-CH), 6.54(d, 2H, Ar-H), 6.93(d, 2H, Ar-H), 8.95(s, 1H, NH), 9.01(s, 1H, OH).

Ethyl 1,4,7,8-tetrahydro-2,7,7-trimethyl-4-(4-nitrophenyl)-5(6H)-oxoquinoline-3-carboxylate (5d). FTIR (KBr, cm⁻¹): 3276, 3210, 3076, 2969, 2902, 1703, 1641, 1530, 1379 cm⁻¹. ¹H NMR (500 MHz, DMSO): δ H (ppm) = 0.83(s, 3H, CH₃), 1.01(s, 3H, CH₃), 1.11(t, 3H, CH₃), 1.96–2.46(m, 4H, 2CH₂), 2.31(s, 3H, CH₃), 3.93–4.0(m, 2H, OCH₂), 4.97(s, 1H, Ar-CH), 7.5–7.61 (m, 4H, Ar-H), 7.97(s, 1H, NH), 9.23(s, 1H, OH).

2-amino-4-(4-nitrophenyl)-7,7-dimethyl-5-oxo-5,6,7,8-tetrahydro-4H-chromene-3-carbonitrile (9c). FTIR(KBr, cm⁻¹): 3403, 3312, 3170, 2969, 2881, 2181, 1668, 1626, 1517, 1345, 856 cm⁻¹. ¹H NMR (500 MHz, DMSO): δ H (ppm) = 0.95(s, 3H, CH₃), 1.04(s, 3H, CH₃), 2.09–2.53(m, 4H, 2CH₂), 4.36(s, 1H, CH), 7.1(s, 2H, NH₂), 7.43–8.17(m, 4H, Ar-H).

2-phenyl-2, 3-dihydro-4(1H)-quinazolinone (13a). FTIR (KBr, cm⁻¹): 3300, 3176, 2981, 1651, 1610, 1507, 1440, 1385, 745 cm⁻¹. ¹H NMR (500 MHz, DMSO): δ H (ppm) = 5.75(s, 1H, CH), 6.67(t, 1H, Ar-H), 6.74(d, 1H, Ar-H), 7.1(s, 1H, NH), 7.23(t, 1H, Ar-H), 7.34(t, 1H, Ar-H), 7.38(t, 1H, Ar-H), 7.49(d, 1H, Ar-H), 7.60(d, 1H, Ar-H), 8.27(s, 1H, CONH).

2-(4-chloro-phenyl)-2, 3-dihydro-1H-quinazolinone (13b). FTIR (KBr, cm⁻¹): 3305, 3184, 3062, 1654, 1606, 1431, 1090, 749 cm⁻¹. ¹H NMR (500 MHz, DMSO): δ H (ppm) = 5.77(s, 1H, CH), 6.68(t, 1H, Ar-H), 6.74(d, 1H, Ar-H), 7.1(s, 1H, NH), 7.24(t, 1H, Ar-H), 7.45(d, 1H, Ar-H), 7.50(d, 1H, Ar-H), 7.61(d, 1H, Ar-H), 8.27(s, 1H, CONH).

Received: 25 April 2021; Accepted: 25 August 2021

Published online: 05 October 2021

References

- Rashidzadeh, A., Ghafuri, H., Esmaili Zand, H. R. & Goodarzi, N. Graphitic carbon nitride nanosheets covalently functionalized with biocompatible vitamin B1: synthesis, characterization, and its superior performance for synthesis of quinoxalines. *ACS Omega* **4**(7), 12544–12554. <https://doi.org/10.1021/acsomega.9b01635> (2019).
- Rahmati, M. & Ghafuri, H. Catalytic Strecker reaction: gC₃N₄-anchored sulfonic acid organocatalyst for the synthesis of α -aminonitriles. *Research on Chemical Intermediates*, 1–14 (2021). <https://www.x-mol.com/paperRedirect/1359656597111214080>
- Zhang, Z., Liu, K., Feng, Z., Bao, Y. & Dong, B. Hierarchical sheet-on-sheet ZnIn₂S₄/gC₃N₄ heterostructure with highly efficient photocatalytic H₂ production based on photoinduced interfacial charge transfer. *Sci. Rep.* **6**, 1–10. <https://doi.org/10.1038/srep19221> (2016).
- Kumar, R., Barakat, M. & Alseroury, F. Oxidized gC₃N₄/polyaniline nanofiber composite for the selective removal of hexavalent chromium. *Sci. Rep.* **7**, 1–11. <https://doi.org/10.1038/s41598-017-12850-1> (2017).
- Dong, G., Zhang, Y., Pan, Q. & Qiu, J. A fantastic graphitic carbon nitride (g-C₃N₄) material: electronic structure, photocatalytic and photoelectric properties. *J. Photochem. Photobiol. C Photochem. Rev.* **20**, 33–50. <https://doi.org/10.1016/j.jphotochemrev.2014.04.002> (2014).
- Wu, Y. *et al.* Electrocatalytic performances of gC₃N₄-LaNiO₃ composite as bi-functional catalysts for lithium-oxygen batteries. *Sci. Rep.* **6**, 1–8. <https://doi.org/10.1038/srep24314> (2016).
- Han, H. *et al.* Cu and boron doped carbon nitride for highly selective oxidation of toluene to benzaldehyde. *Molecules* **20**, 12686–12697. <https://doi.org/10.3390/molecules200712686> (2015).
- Davarpanah, J., Ghahremani, M. & Najafi, O. Synthesis of 1, 4-dihydropyridine and polyhydroquinoline derivatives via Hantzsch reaction using nicotinic acid as a green and reusable catalyst. *J. Mol. Struct.* **1177**, 525–535. <https://doi.org/10.1016/j.molstruc.2018.10.002> (2019).
- Kusampally, U., Dhachapally, N., Kola, R. & Kamatala, C. R. Zeolite anchored Zr-ZSM-5 as an eco-friendly, green, and reusable catalyst in Hantzsch synthesis of dihydropyridine derivatives. *Mater. Chem. Phys.* **242**, 122497. <https://doi.org/10.1016/j.matchemphys.2019.122497> (2020).
- Alponti, L. H., Picinini, M., Urquieta-Gonzalez, E. A. & Corrêa, A. G. USY-zeolite catalyzed synthesis of 1,4-dihydropyridines under microwave irradiation: Structure and recycling of the catalyst. *J. Mol. Struct.* **1227**, 129430. <https://doi.org/10.1016/j.molstruc.2020.129430> (2021).
- Das, D. Multicomponent reactions in organic synthesis using copper-based nanocatalysts. *ChemistrySelect* **1**, 1959–1980. <https://doi.org/10.1002/slct.201600414> (2016).
- Domling, A., Wang, W. & Wang, K. Chemistry and biology of multicomponent reactions. *Chem. Rev.* **112**, 3083–3135. <https://doi.org/10.1021/cr100233r> (2012).
- Khazaei, A., Moosavi-Zare, A. R., Mohammadi, Z., Khakyzadeh, V. & Afsar, J. Nano-TiO₂ as an efficient catalyst for tandem Knoevenagel–Michael-cyclocondensation reaction of dimedone with aromatic aldehydes and ammonium acetate or aromatic amines under solvent-free conditions. *J. Chin. Chem. Soc.* **63**, 165–170. <https://doi.org/10.1002/jccs.201500384> (2016).
- Aute, D., Kshirsagar, A., Uphade, B. & Gadhave, A. Aluminized polyborate-catalysed green and efficient synthesis of polyhydroquinolines under solvent-free conditions. *Res. Chem. Intermed.* **46**, 3491–3508. <https://doi.org/10.1007/s11164-020-04158-z> (2020).
- Zhang, Q., Ma, X.-M., Wei, H.-X., Zhao, X. & Luo, J. Covalently anchored tertiary amine functionalized ionic liquid on silica coated nano-Fe₃O₄ as a novel, efficient and magnetically recoverable catalyst for the unsymmetrical Hantzsch reaction and Knoevenagel condensation. *RSC Adv.* **7**, 53861–53870. <https://doi.org/10.1039/C7RA10692K> (2017).
- Kiyani, H. & Ghorbani, F. Boric acid-catalyzed multi-component reaction for efficient synthesis of 4H-isoxazol-5-ones in aqueous medium. *Res. Chem. Intermed.* **41**, 2653–2664. <https://doi.org/10.1007/s11164-013-1411-x> (2015).
- Yü, S.-J., Wu, S., Zhao, X.-M. & Lü, C.-W. Green and efficient synthesis of acridine-1,8-diones and hexahydroquinolines via a KH₂PO₄ catalyzed Hantzsch-type reaction in aqueous ethanol. *Res. Chem. Intermed.* **43**, 3121–3130. <https://doi.org/10.1007/s11164-016-2814-2> (2017).
- Zhang, Q., Wei, H., Li, J., Zhao, X. & Luo, J. One-pot synthesis of benzopyrans catalyzed by silica supported dual acidic ionic liquid under solvent-free conditions. *Heterocycl. Commun.* **23**, 411–414. <https://doi.org/10.1515/hc-2017-0163> (2017).
- Lu, J., Fu, X., Zhang, G. & Wang, C. β -Cyclodextrin as an efficient catalyst for the one-pot synthesis of tetrahydrobenzo [b] pyran derivatives in water. *Res. Chem. Intermed.* **42**, 417–424. <https://doi.org/10.1007/s11164-015-2027-0> (2016).
- Malviya, J., Kala, S., Sharma, L. & Singh, R. Efficient three-component one-pot synthesis of 4 H-Pyrans. *Russ. J. Org. Chem.* **55**, 686–693. <https://doi.org/10.1134/S1070428019050178> (2019).
- Mirjalili, B. B. F., Zaghaghi, Z. & Monfared, A. Synthesis of 2,3-dihydroquinazolin-4 (1H)-ones in the presence of Fe₃O₄@nanocellulose–OPO₃H as a bio-based magnetic nanocatalyst. *J. Chin. Chem. Soc.* **67**, 197–201. <https://doi.org/10.1002/jccs.201900264> (2020).
- Rao, A. D. *et al.* Sulfonic acid functionalized Wang resin (Wang-OSO₃H) as polymeric acidic catalyst for the eco-friendly synthesis of 2,3-dihydroquinazolin-4 (1H)-ones. *Tetrahedron Lett.* **56**, 4714–4717. <https://doi.org/10.1080/00397911.2016.1213850> (2015).
- Pan, S. *et al.* MCM-41@ Schiff base-Co (OAc) 2 as an efficient catalyst for the synthesis of pyran derivatives. *Res. Chem. Intermed.* **46**, 1353–1371. <https://doi.org/10.1080/00397911.2016.1213850> (2020).
- Hong, M. & Cai, C. Ytterbium(III) bis (perfluorooctanesulfonyl) imide catalyzed one-pot synthesis of tetrahydrobenzo [b] pyrans in fluorosol biphasic system. *J. Chem. Res.* **34**, 568–570. <https://doi.org/10.3184/030823410X12863845344182> (2010).
- Tamoradi, T., Ghadermazi, M. & Ghorbani-Choghmarani, A. Synthesis of polyhydroquinoline, 2,3-dihydroquinazolin-4 (1H)-one, sulfide and sulfoxide derivatives catalyzed by new copper complex supported on MCM-41. *Catal. Lett.* **148**, 857–872. <https://doi.org/10.1007/s10562-018-2311-x> (2018).
- Mekala, R. *et al.* Efficient synthesis of 2, 3-dihydroquinazolin-4 (1H)-ones catalyzed by titanium silicon oxide nanopowder in aqueous media. *Synth. Commun.* **47**, 121–130. <https://doi.org/10.1080/00397911.2016.1254801> (2017).
- Khan, A. A., Mitra, K., Mandal, A., Baildya, N. & Mondal, M. A. Yttrium nitrate catalyzed synthesis, photophysical study, and TD-DFT calculation of 2,3-dihydroquinazolin-4 (1H)-ones. *Heteroat. Chem.* **28**, e21379. <https://doi.org/10.1002/hc.21379> (2017).
- Guo, X., Duan, J., Li, C., Zhang, Z. & Wang, W. Highly efficient Z-scheme gC₃N₄/ZnO photocatalysts constructed by co-melting-recrystallizing mixed precursors for wastewater treatment. *J. Mater. Sci.* **55**, 2018–2031. <https://doi.org/10.1007/s10853-019-04097-0> (2020).
- Yang, X., Tang, B., Wu, T. & Cao, X. g-C₃N₄/TiO₂ composite photocatalyst and its application to asphalt for NO removal. *J. Mater. Civ. Eng.* **31**, 04019141. <https://doi.org/10.1061/%28ASCE%29MT.1943-5533.0002763> (2019).
- Li, X. *et al.* Synergistic effect of efficient adsorption g-C₃N₄/ZnO composite for photocatalytic property. *J. Phys. Chem. Solids* **75**, 441–446. <https://doi.org/10.1016/j.jpcs.2013.12.001> (2014).
- Rahmati, M., Ghafuri, H., Ghanbari, N. & Tajik, Z. 1,4-butanediol functionalized graphitic carbon nitride: efficient catalysts for the one-pot synthesis of 1,4-dihydropyridine and polyhydroquinoline derivative through Hantzsch reaction. *Polycycl. Arom. Compd.* <https://doi.org/10.1080/10406638.2020.1852583> (2020).

32. Maleki, A., Eskandarpour, V., Rahimi, J. & Hamidi, N. Cellulose matrix embedded copper decorated magnetic bionanocomposite as a green catalyst in the synthesis of dihydropyridines and polyhydroquinolines. *Carbohydr. Polym.* **208**, 251–260. <https://doi.org/10.1016/j.carbpol.2018.12.069> (2019).
33. Brahmachari, G., Laskar, S. & Banerjee, B. Eco-friendly, one-pot multicomponent synthesis of pyran annulated heterocyclic scaffolds at room temperature using ammonium or sodium formate as non-toxic catalyst. *J. Heterocycl. Chem.* **51**, E303–E308. <https://doi.org/10.1002/jhet.1974> (2014).
34. Qareaghaj, O. H., Mashkouri, S., Naimi-Jamal, M. R. & Kaupp, G. Ball milling for the quantitative and specific solvent-free Knoevenagel condensation+ Michael addition cascade in the synthesis of various 2-amino-4-aryl-3-cyano-4 H-chromenes without heating. *RSC Adv.* **4**, 48191–48201. <https://doi.org/10.1039/C4RA06603K> (2014).
35. Dekamin, M. G. & Eslami, M. Highly efficient organocatalytic synthesis of diverse and densely functionalized 2-amino-3-cyano-4 H-pyrans under mechanochemical ball milling. *Green Chem.* **16**, 4914–4921. <https://doi.org/10.1039/C4GC00411F> (2014).
36. Ghafari, H., Goodarzi, N., Rashidizadeh, A. & Fard, M. A. D. ompg-C 3 N 4/SO 3 H: an efficient and recyclable organocatalyst for the facile synthesis of 2, 3-dihydroquinazolin-4 (1 H)-ones. *Res. Chem. Intermed.* **45**, 5027–5043 (2019).
37. Pourhasan-Kisomi, R., Shirini, F. & Golshekan, M. Introduction of organic/inorganic Fe₃O₄@MCM-41@ Zr-piperazine magnetite nanocatalyst for the promotion of the synthesis of tetrahydro-4H-chromene and pyrano [2,3-d] pyrimidinone derivatives. *Appl. Organomet. Chem.* **32**, e4371. <https://doi.org/10.1002/aoc.4371> (2018).
38. Zhang, Q., Gao, Y.-H., Qin, S.-L. & Wei, H.-X. Facile one-pot synthesis of amidoalkyl naphthols and benzopyrans using magnetic nanoparticle-supported acidic ionic liquid as a highly efficient and reusable catalyst. *Catalysts* **7**, 351. <https://doi.org/10.3390/catal7110351> (2017).
39. Khodabakhshi, M. R., Kiamehr, M. & Karimian, R. Efficient one-pot synthesis of 1,4-dihydropyridine and polyhydroquinoline derivatives using sulfanilic acid-functionalized boehmite nano-particles as an organic-inorganic hybrid catalyst. *Polycyclic Aromat. Compd.* 1–15. <https://doi.org/10.1080/10406638.2021.1884100> (2021).
40. Karhale, S., Bhenki, C., Rashinkar, G. & Helavi, V. Covalently anchored sulfamic acid on cellulose as heterogeneous solid acid catalyst for the synthesis of structurally symmetrical and unsymmetrical 1, 4-dihydropyridine derivatives. *New J. Chem.* **41**, 5133–5141. <https://doi.org/10.1039/C7NJ00685C> (2017).
41. Tekale, S. U., Munde, S. B., Kauthale, S. S. & Pawar, R. P. An efficient, convenient, and solvent-free synthesis of 2,3-dihydroquinazolin-4 (1 H)-ones using montmorillonite-KSF clay as a heterogeneous catalyst. *Org. Prep. Proced. Int.* **50**, 314–322. <https://doi.org/10.1080/00304948.2018.1462058> (2018).

Acknowledgements

We are grateful for the financial support from The Research Council of Iran University of Science and Technology (IUST), Tehran, Iran.

Author contributions

All authors reviewed the manuscript.

Competing interests

The authors declare no competing interests.

Additional information

Supplementary Information The online version contains supplementary material available at <https://doi.org/10.1038/s41598-021-97360-x>.

Correspondence and requests for materials should be addressed to H.G.

Reprints and permissions information is available at www.nature.com/reprints.

Publisher's note Springer Nature remains neutral with regard to jurisdictional claims in published maps and institutional affiliations.



Open Access This article is licensed under a Creative Commons Attribution 4.0 International License, which permits use, sharing, adaptation, distribution and reproduction in any medium or format, as long as you give appropriate credit to the original author(s) and the source, provide a link to the Creative Commons licence, and indicate if changes were made. The images or other third party material in this article are included in the article's Creative Commons licence, unless indicated otherwise in a credit line to the material. If material is not included in the article's Creative Commons licence and your intended use is not permitted by statutory regulation or exceeds the permitted use, you will need to obtain permission directly from the copyright holder. To view a copy of this licence, visit <http://creativecommons.org/licenses/by/4.0/>.

© The Author(s) 2021